

Titin-truncating variants affect heart function in disease cohorts and the general population

Article

Accepted Version

Schafer, S., de Marvao, A., Adami, E., Fiedler, L. R., Ng, B., Khin, E., Rackham, O. J. L., van Heesch, S., Pua, C. J., Kui, M., Walsh, R., Tayal, U., Prasad, S. K., Dawes, T. J. W., Ko, N. S. J., Sim, D., Chan, L. L. H., Chin, C. W. L., Mazzarotto, F., Barton, P. J., Kreuchwig, F., de Kleijn, D. P. V., Totman, T., Biffi, C., Tee, N., Rueckert, D., Schneider, V., Faber, A., Regitz-Zagrosek, V., Seidman, J. G., Seidman, C. E., Linke, W. A., Kovalik, J.-P., O'Regan, D., Ware, J. S., Hubner, N. and Cook, S. A. (2017) Titin-truncating variants affect heart function in disease cohorts and the general population. *Nature Genetics*, 49 (1). pp. 46-53. ISSN 1546-1718 doi: <https://doi.org/10.1038/ng.3719> Available at <https://centaur.reading.ac.uk/68801/>

It is advisable to refer to the publisher's version if you intend to cite from the work. See [Guidance on citing](#).

Published version at: <http://dx.doi.org/10.1038/ng.3719>

To link to this article DOI: <http://dx.doi.org/10.1038/ng.3719>

Publisher: Nature Publishing Group

All outputs in CentAUR are protected by Intellectual Property Rights law, including copyright law. Copyright and IPR is retained by the creators or other copyright holders. Terms and conditions for use of this material are defined in the [End User Agreement](#).

www.reading.ac.uk/centaur

CentAUR

Central Archive at the University of Reading

Reading's research outputs online

Titin truncating variants affect the heart in health and disease

Schafer S^{1,2*}, de Marvao A^{3*}, Adami E⁴, Fiedler L², Ng B¹, Khin E², Rackham O², van Heesch S⁴, Pua CJ¹, Kui M², Walsh R⁵, Tayal U⁵, Prasad SK⁵, Dawes TJW³, Ko NSJ², Sim D¹, Chan LL¹, Chin, CW¹, Mazzarotto F⁵, Barton PJ⁵, Kreuchwig F⁴, de Kliejn D⁶, Totman T⁶, Biffi C³, Tee N¹, Schneider V⁴, Faber A⁴, Regitz-Zagrosek V⁷, Seidman JG⁸, Seidman CE^{8,9,10}, Linke WA¹¹, Kovalik JP², O'Regan DP³, Ware JS^{3,5**}, Hubner N^{4,12,13**}, Cook SA^{2,1,5**¶}

¹National Heart Centre Singapore, Singapore.

²Duke-National University of Singapore, Singapore.

³Medical Research Council Clinical Sciences Centre, Faculty of Medicine, Imperial College London, Hammersmith Hospital Campus, Du Cane Road, London, W12 0HS, England

⁴Cardiovascular and Metabolic Sciences, Max-Delbrück-Center for Molecular Medicine (MDC), Robert-Rossle-Strasse 10, 13125 Berlin, Germany.

⁵National Heart and Lung Institute & NIHR Royal Brompton Cardiovascular BRU, Imperial College London, London, UK.

⁶Department of Surgery, National University of Singapore, Singapore

⁷Institute of Gender in Medicine, Charité Universitaetsmedizin Berlin, and German Center for Cardiovascular Research, Berlin, Germany.

⁸Department of Genetics, Harvard Medical School, Boston, MA 02115, USA.

⁹Division of Cardiovascular Medicine, Brigham and Women's Hospital, Boston, MA 02115, USA.

¹⁰Howard Hughes Medical Institute, Chevy Chase, MD 20815, USA.

¹¹Department of Cardiovascular Physiology, Ruhr University Bochum, Germany.

¹²DZHK (German Centre for Cardiovascular Research), partner site Berlin, Germany.

¹³Charité-Universitätsmedizin, Berlin, Germany.

^{*}, Co-first authors

^{**}, Co-senior authors

[¶], corresponding author

Abstract

Titin truncating variants (TTNtv) commonly cause dilated cardiomyopathy (DCM). However, TTNtv are also encountered in ~1% of the general population but potentially silent, perhaps reflecting position-dependent allelic factors. To better understand TTNtv we integrated *TTN* allelic series, cardiac imaging and genomic data from human cohorts and studied rat models with disparate TTNtv. In patients with DCM, TTNtv throughout the *TTN* molecule were significantly associated with DCM, although more strongly so (odds ratio ~50) when located in the A-band. Ribosomal profiling in rat revealed the translational footprint of premature stop codons in *Ttn* and showed TTNtv position-independent nonsense-mediated degradation of the mutant allele and a signature of perturbed cardiac metabolism. Heart physiology in TTNtv rats was unremarkable at baseline but became impaired during cardiac stress. In healthy humans, TTNtv were associated with eccentric cardiac remodelling, which is a feature of DCM. These data show that TTNtv have molecular and physiological effects on the heart across species, with a continuum of expressivity in health and disease.

Dilated cardiomyopathy (DCM) has a prevalence of up to 1:250¹, is the commonest indication for heart transplantation and is often associated with titin truncating variants (TTNtv, 15-20% of DCM cases), which are enriched in the *TTN* A-band^{2,3}. A surprising ~1% of the general population has a TTNtv in the absence of DCM, which has stimulated much debate as to the pathogenicity of TTNtv⁴⁻⁷. It has been suggested that TTNtv in the healthy population may be phenotypically silent and that TTNtv that segregate in familial DCM are perhaps modifiers of other DCM-causing variants³. However, it is also known that genetic variation affecting disease genes can be associated with quantitative variation in the physiology of healthy individuals⁸, which has not been assessed formally for TTNtv.

We showed previously that *TTN* exon characteristics are important determinants of TTNtv pathogenicity. Variants encoded in exons that are not spliced into *TTN* isoforms expressed in the heart (non-cardiac exons with 'Percent Spliced In' (PSI) < 15%) are not associated with DCM³, while variants encoded in exons that only incorporate into the N2BA and not into the N2B isoform have weak associations with disease. In studies of human induced pluripotent stem cell (iPSC)-derived cardiomyocytes (iPSC-CMs)⁹ alternative exon splicing is a major mechanism for reduced penetrance for some I-band TTNtv. When taking only TTNtv that are located in cardiac exons (PSI > 15%) into account, approximately 0.5% of the general population have a TTNtv that might be expected to cause DCM but does not.

In addition to the complexities surrounding TTNtv penetrance, the molecular mechanisms underlying TTNtv are uncharacterized. Nonsense-mediated decay (NMD) of the mutated allele by RNA-seq or a reduction in full-length TTN by agarose gel analysis has not been demonstrated, which if documented would support a haploinsufficient disease mechanism^{3,9,10}. Equally, accumulation of a truncated TTN protein molecule is not apparent in human heart samples³ and is rarely present in iPSC-CMs⁹ suggesting a poison-peptide/dominant negative mechanism to be unlikely.

Here, we undertook studies of DCM patients, rat models of TTNtv and human volunteers from the general population to better understand TTNtv pathogenicity and molecular effect with a specific focus on dissecting a hypothesized position-dependent penetrance effect of TTNtv alleles. To do this, we performed a meta-analysis of TTNtv in DCM patients ($n = 2,495$) as compared to controls ($n = 61,834$) and generated two rat models of TTNtv with mutations at opposite ends of the *Ttn* molecule. We integrated RNA-sequencing (RNA-seq) and ribosome profiling (Ribo-seq) data across models and species and performed metabolic and signaling studies to outline potential disease mechanisms. To define the effects of TTNtv on the heart in the general population we combined 2D and 3D cardiac magnetic resonance imaging (CMR) with *TTN* sequencing in healthy volunteers ($n = 1,409$).

Results

TTNtv in constitutive exons across the *TTN* molecule from the Z-disc to the M-band are associated with DCM

We and others have shown that A-band TTNtv are associated with DCM^{2,3,9} but the association of DCM with TTNtv in the I-band, Z-disc or the M-line has not been demonstrated and it is suggested that proximal TTNtv, in particular, may be non-penetrant. To address variant effect across the *TTN* molecule we retrieved TTNtv alleles from DCM patients from available sources, combined these data with novel DCM cases ($n = 1,105$) and performed a meta-analysis using ExAC¹¹ and other controls (cohort totals: DCM ($n = 2,495$) controls ($n = 61,834$); see Methods). This showed that TTNtv in constitutive exons (PSI > 90%) are significantly associated with DCM irrespective of their position in *TTN* (Table 1).

While some I-band TTNtv may be rescued by differential splicing⁹, we observed that I-band TTNtv in constitutive cardiac exons were significantly associated with DCM, which was true for both proximal and distal I-band variants. TTNtv in Z-disc exons were also associated with DCM, although with a much lower odds ratio (OR: 5.3) than A-band TTNtv (OR: 49.8). It has been proposed that a distal internal promoter of the *Cronos* *TTN* isoform¹², which we confirmed to be present in adult human heart using Cap Analysis of Gene Expression (CAGE)¹³ data (Fig S1), can rescue proximal TTNtv effect. However, we found that proximal TTNtv are also penetrant and associated with DCM. By splitting regions of titin into protein regions (Table 1), or consecutive uniformly-sized bins ($n = 40$, (Fig S2)) we were able to show the proportion of truncations that are penetrant (etiologic fraction) in regions of *TTN* upstream of the *Cronos* promoter is comparable to the proportion in the downstream A-Band. These data show that distal I-band and all A-band TTNtv have larger ORs than very proximal or distal variants, which suggests position-dependent effects for the penetrance of TTNtv in DCM.

Table 1. Meta-analysis shows an association of TTNtv in constitutive exons throughout the gene with DCM. Exon usage are displayed base on the levels of PSI¹⁴. Constitutive exons are spliced into titin isoforms with an efficiency of at least 90%. OR, odds ratio. EF, etiologic fraction. *P*-values indicate significant enrichment for TTNtv in DCM (binomial test).

	DCM Positive (n=2,495)	Control Positive (n=61,834)	DCM Prevalence (%)	Control Prevalence (%)	OR	OR (hi)	OR (lo)	EF	<i>P</i> -value
Sarcomere domain affected by variant									
A-band (constitutive)	268	149	10.74	0.24	49.8	61.1	40.6	0.98	2.4×10^{-260}
I-band (Distal constitutive Post-Cronos)	9	7	0.36	0.01	32.0	85.9	11.9	0.97	2.5×10^{-9}
I-band (Distal constitutive Pre-Cronos)	18	23	0.72	0.04	19.5	36.2	10.5	0.95	6.6×10^{-15}
I-band (Non-constitutive)	6	102	0.24	0.17	1.5	3.3	0.6	0.31	0.46
I-band (Proximal constitutive)	22	29	0.88	0.05	19.0	33.0	10.9	0.95	1.1×10^{-17}
M-band (constitutive)	6	40	0.24	0.07	3.7	8.8	1.6	0.73	0.01
Z-disc (constitutive)	7	33	0.28	0.05	5.3	11.9	2.3	0.81	0.001
Z-disc (Non-constitutive)	0	11	0.00	0.02	NA	NA	NA	NA	NA

Premature stop codons cause nonsense-mediated RNA decay and disrupt translation of full length, sarcomere-spanning *Ttn*

Our meta-analyses of DCM patients showed that TTNtv throughout the *TTN* molecule are penetrant but have variable, position-related odds ratios. To study putative position-dependent effects in greater detail while controlling for other genetic and non-genetic factors we modelled proximal and distal TTNtv in two independent rat strains on the same genetic background (TTNtvA: with variation in the A-band; TTNtvZ: with variation in the Z-disc; for details see Fig S3). Animals with homozygous mutations were not viable, as previously described for TTNtv in the mouse¹⁰ while heterozygous animals were born in normal Mendelian ratios (data not shown).

We bred TTNtv heterozygous rats on a F344 background with *Ttn* wild type Brown Norway rats to obtain an F1 cross to specifically enable allele-specific analysis of *Ttn* transcription and translation in the heart using RNA-seq and Ribo-seq (Fig 1a and Fig S4)^{15,16}. Ribosome protected fragments (RPFs) showed clear trinucleotide periodicity across the transcriptome, indicating actively translating ribosomes (Fig 1b). *Ttn* transcripts with a truncation in the A-band were transcribed and translated as far as the premature nonsense codon, which efficiently stopped translation thereafter (Fig 1c,d).

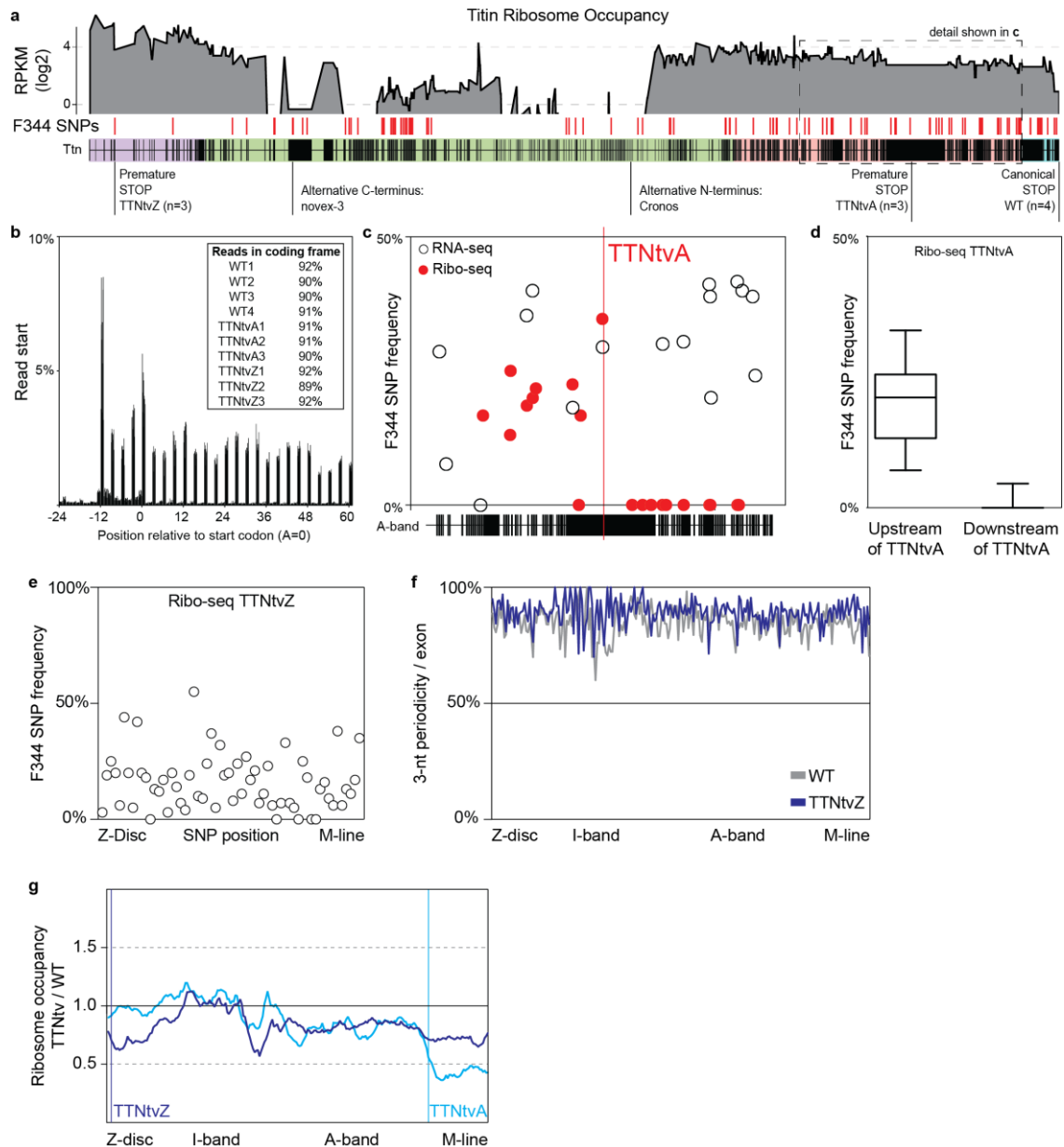


Fig 1. Ribosome profiling reveals the translational footprint of truncating variants in *Ttn*. **a** Ribosome occupancy across *Ttn*: Average reads per kilobase per million mapped reads (RPKM) per exon for 10 BN/F344 F1 rats. F344 SNPs on the BN background (n=121) allow assessment of allele-specific translation for 2 distinct models of truncations and *Ttn* wild type animals. Proximal and distal truncations affect different isoform populations of *Ttn*. Purple indicates Z-disc, green I-band, pink A-band and blue M-line. **b** Ribo-seq reads (28-mers) show clear 3-nt periodicity across the genome for all replicates indicating that the datasets effectively capture actively translating ribosomes in the heart at a high resolution. **c,d** Ribosomes occupy the F344 allele in TTNtvA animals upstream of the premature stop codon in the A-band of *Ttn* exposing the synthesis of truncated *Ttn* isoforms. The premature stop efficiently releases ribosomes from the mutant *Ttn* message. *Ttn* protein synthesized after TTNtvA is exclusively generated from the healthy BN allele (Whiskers show 10-90 percentile). Allele frequencies in both RNA-seq and Ribo-seq were consistently below 50%, indicative for NMD. **e** F344 SNPs located after TTNtvZ are occupied by ribosomes, indicating translation after the proximal truncation in *Ttn*. **f** Ribo-seq reads located downstream of TTNtvZ do not lower 3-nt periodicity across exons suggesting that they actively translate canonical *Ttn* sequence at similar levels as animals with two wild type *Ttn* alleles. **g** TTNtvZ reduces ribosome density initially but translation of *Ttn* is gradually rescued after the frameshift in the Z-disc. Translation of A-band exons, but not of I-band exons, is reduced in mutants compared to WT animals. TTNtvA efficiently reduces translation after the premature stop codon.

The premature stop codon of the TTNtvZ allele did not prevent translation downstream of the non-canonical stop and F344 SNPs encoded on the truncated *Ttn* allele were detected throughout *Ttn* (Fig. 1e). Rescue of translation from the truncated F344 allele did not decrease the 3-nt periodicity across *Ttn* when compared to F1 wild type (WT) animals that synthesize *Ttn* from two healthy alleles (Fig. 1f). Exon-level analyses showed that the TTNtvZ variant initially reduces ribosome occupancy at

the N-terminus of *Ttn* (~50% that of WT) but subsequently translation is partially recovered (Fig 1g). This apparent rescue of translation might be explained in parts by internal ribosomal entry sites, transcription start sites that generate *Ttn* isoforms with alternative N-termini and potentially by factors that maintain ribosomes on the huge *Ttn* molecule during its translation. In support of this, human CAGE data¹³ and epigenetic marks¹⁷ revealed distal *TTN* promoters in the human heart (Fig S1), as previously suggested¹². In TTNtvA animals, we only detected ribosomes on the healthy BN allele after the premature stop codon (Fig 1c). This led to a decrease of ribosome occupancy by 50% when we compared to WT animals that still translate this section of titin from both alleles (Fig 1g).

In both mutant rats there was a relative increase in exon translation in the I-band (Fig. 1g) that reflects differential *Ttn* mRNA processing and higher PSI ratios¹⁴ of exons in the I-band, as observed in human iPS-derived cardiomyocytes with TTNtv⁹. This is indicative of an increase in N2BA isoform expression in TTNtv carriers. To translate this finding, we compared cardiac RNA-seq data³ from DCM patients either with ($n = 17$) or without ($n = 91$) a TTNtv and observed similar patterns of alternative splicing as seen in the rat models (Fig 2a). Allele-specific RNA-seq data revealed a slight upregulation of the WT allele and profound NMD of the allele carrying the TTNtv in both the TTNtvA and the TTNtvZ models (Fig 2b). These data demonstrate a multi-allelic effect of TTNtv on the overall *TTN* isoform composition across species (that can cause DCM^{18,19}), and that TTNtv confer position-independent NMD.

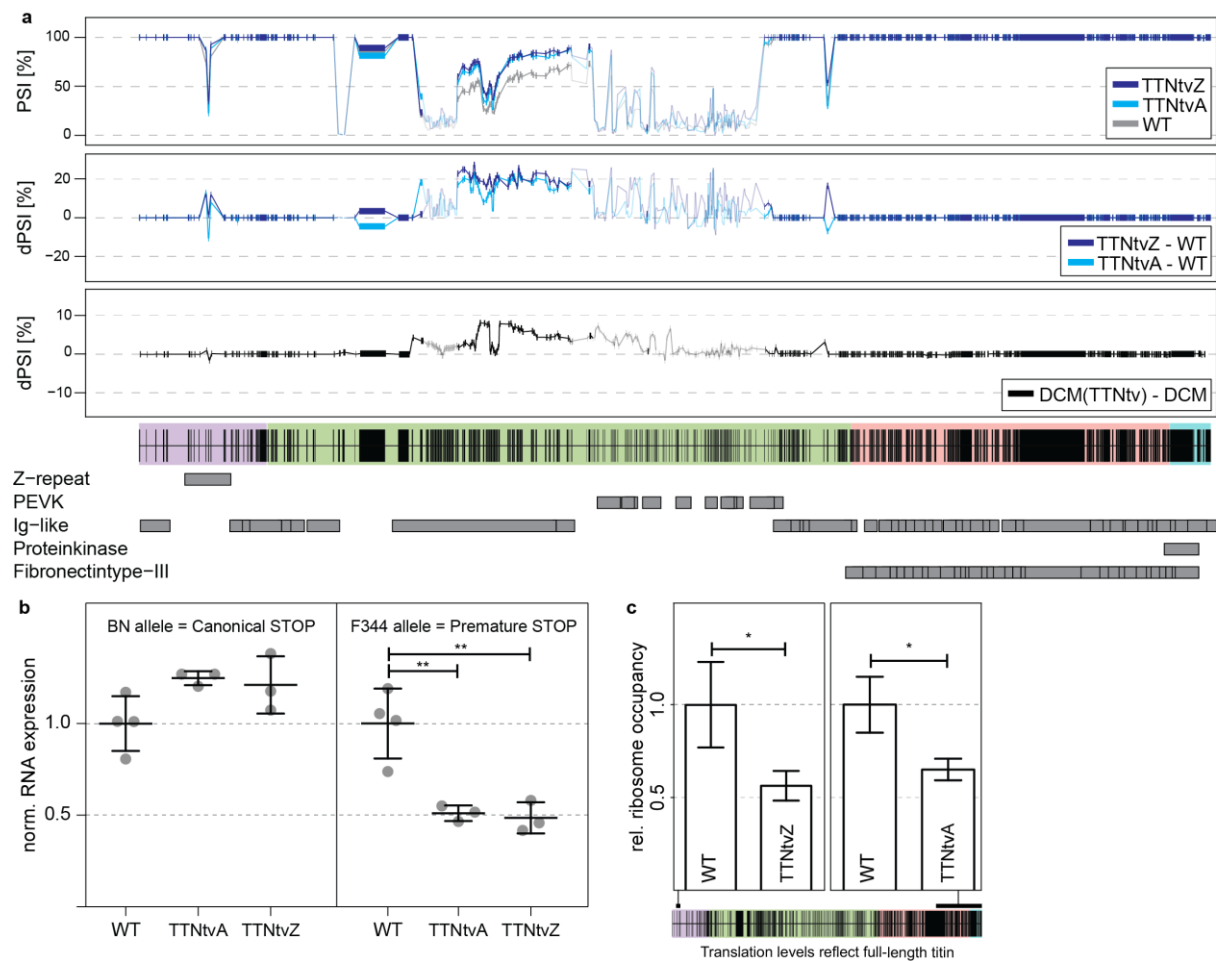


Fig 2. Proximal and distal truncations in titin alter isoform processing and trigger NMD. **a** PSI and deltaPSI of titin exons expressed in the heart for TTNtvA, TTNtvZ and WT animals and human DCM. Exons with at least 10 inclusion reads are marked in solid colours. Truncating mutations in titin activate splicing in of I-band exons in the TTNtv rat models and also human DCM patients that carry *TTN* truncations. **b** RNA-seq reads assigned to either BN or F344 alleles: TTNtv selectively trigger nonsense-mediated decay of truncated *Ttn* transcripts. **c** Ribo-seq expression of exons that are exclusively being synthesized in TTNtvA and TTNtvZ animals reveal that both TTNtv models generate 60% of full-length titin compared to WT. Purple indicates Z-disc, green I-band, pink A-band and blue M-line. *P < 0.05; **P < 0.01.

It was noticeable that both the proximal and the distal TTNtv triggered NMD with identical efficiencies irrespective of their location in the *Ttn* molecule. The fact that the proximal truncation triggers NMD indicates that the premature stop codon close to the N-terminus in the TTNtvZ is functional and that ribosomes cannot clear exon-exon junction complexes^{20,21}. Assessing translation beyond the truncation in the TTNtvA model and within the 4-exon deletion in TTNtvZ revealed that both rat models synthesize lesser amounts (~60% of WT rats) of full-length, sarcomere-spanning Ttn (Fig 2c). In keeping with our published data³, protein gel electrophoresis did not identify a truncated Ttn isoform or a reduction in the Ttn:Mhc ratio in mutant rat heart (Fig S5). This suggests rapid turnover of mutant protein that, for the first time, we document the existence of by showing its synthesis (Fig 1). It also shows that while there are significantly less ribosomes translating full length protein, TTN protein changes are not apparent at the resolution of gel analysis. Overall changes in full length TTN protein might be compensated not just by an upregulation of the wildtype allele ($P = 0.02$; Fig 2b), but also via an increase in ribosome translational speed or changes in protein-turnover.

Taken together these data show that proximal and distal *Ttn* truncations disrupt Ttn protein synthesis but have different translational footprints. However, their effect on NMD of the sarcomere-spanning *Ttn* isoforms is similar and leads to identical reductions in full-length Ttn expression.

Titin truncations cause position-independent perturbation of cardiac metabolism and signaling

To determine whether distinct or similar molecular phenotypes are associated with proximal or distal TTNtv, we performed pathway analysis²² of the genome-wide transcription (RNA-seq) and translation (Ribo-seq) profiles of TTNtvZ and TTNtvA as compared to controls. The gene expression differences observed between TTNtv animals and WT controls were highly correlated for TTNtvA and TTNtvZ both for RNA-seq and also Ribo-seq data, showing both mutant strains to have similarly perturbed transcriptomes ($R^2 = 0.841$; $P < 0.0001$) and translomes ($R^2 = 0.837$; $P < 0.0001$; see also Fig S6 & Table S1). Gene set enrichment analyses showed significantly overlapping KEGG^{22,23} terms between TTNtv animals when compared to WT (RNA-seq P value $< 10^{-15}$; Ribo-seq P value $< 10^{-15}$; Pearson Chi-square test; Fig 3a), which suggested altered cardiac metabolism that was independent of the position of the TTNtv.

To investigate further the molecular signatures of altered cardiac metabolism in mutant animals, we performed quantitative metabolomic profiling of WT and TTNtv hearts. Liquid chromatography mass spectrometry (LC-MS) showed reduced amounts of medium and long chain fatty acid acyl-carnitines in TTNtv hearts as compared to controls (Fig 3b; Table S2). We also performed capillary electrophoresis mass spectrometry, complementary to LC-MS, and observed accumulation of alternative myocardial substrates (branched-chain amino acid metabolites and glycolytic intermediates; Fig 3c-e; Fig S7) in mutants. These changes are similar to those seen in the failing heart and the pressure-loaded non-failing heart^{24,25} and are associated with a shift in cardiac metabolism away from fatty acids and towards glycolysis, which may be adaptive^{26–28}. There was no change in the major energy substrates (e.g. ATP; Fig S8), which are only diminished in advanced cardiac failure²⁹.

The signaling changes in the heart due to TTNtv are likely many. We found that variation in metabolic proteins interacting with TTN, such as FHL2 (Fig S9), are small and their functional role cannot be established based on these data alone. It is known that mTORC1 signaling is activated in familial DCM³⁰ and its activity is detrimental in a mouse model of DCM due to *LMNA* mutation³¹. We profiled the mTORC1 pathway in the TTNtv rat hearts, where metabolites that activate mTOR³² are elevated (Fig 3) and observed activation of this pathway (Fig S10). The relative importance of these signaling variations for DCM pathobiology remain to be established.

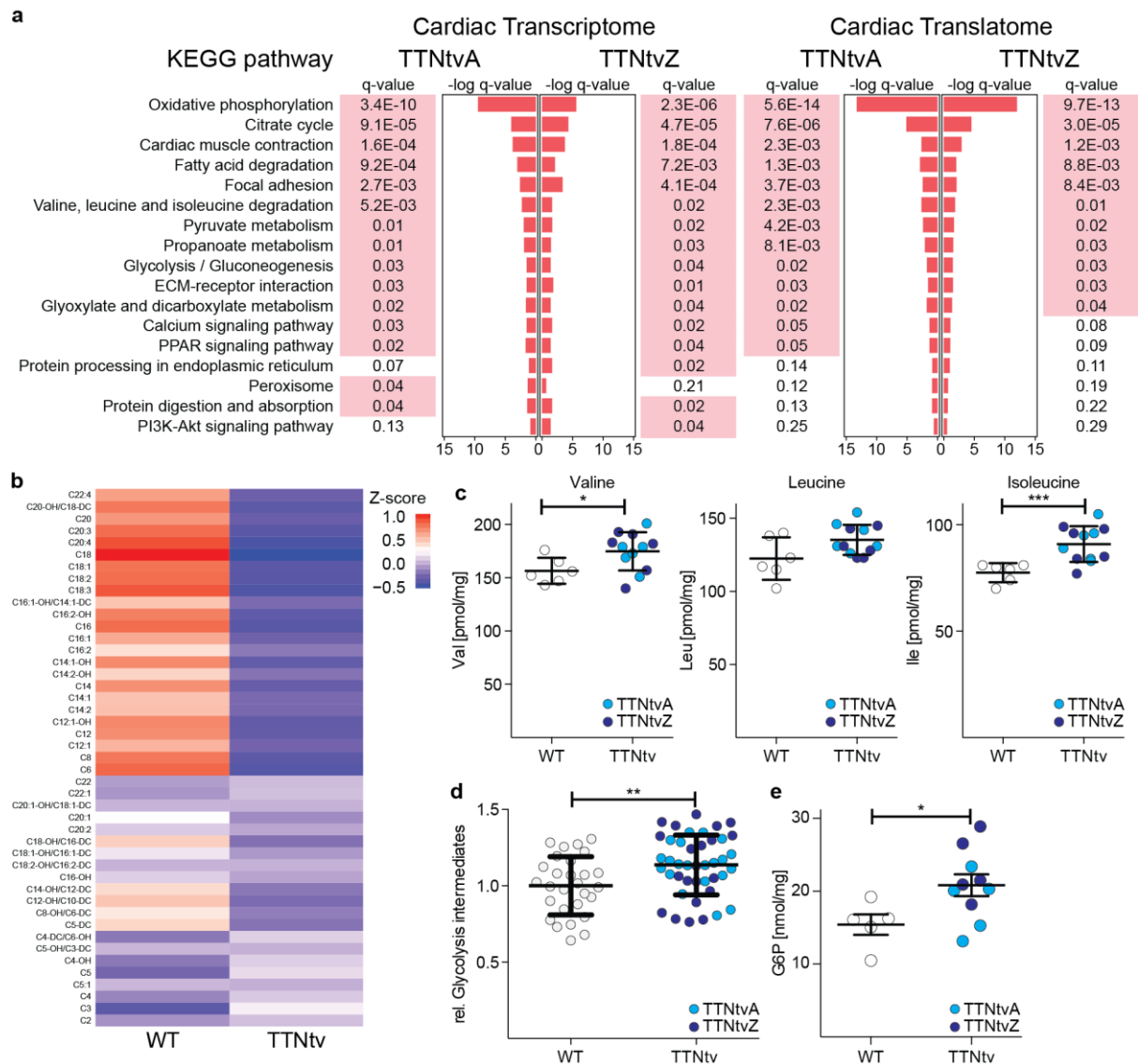


Fig 3. Hearts with proximal and distal truncations in titin undergo metabolic reprogramming. **a** Pathway analyses based on RNA-seq and Ribo-seq data suggest perturbed metabolism, structural integrity and mechano-sensation of the TTNtv heart. This molecular signature is strikingly similar in rats with proximal and distal truncations (P value $< 10^{-15}$; Pearson Chi-square test). **b** Unsupervised clustering by k-means of cardiac fatty acid acylcarnitine abundance in WT ($n=5$) and TTNtv ($n=10$) rats. -OH and -DC designate hydroxylated and dicarboxylic acid acylcarnitine species respectively. Metabolite profiles showing **c** branched chain amino acids (valine, leucine and isoleucine), **d** sum of measured glycolytic intermediates (metabolites are detailed in **Table S3**) and **e** glucose-6-phosphate (G6P) in cardiac tissue of WT ($n=6$) and TTNtv ($n=12$) rats. For individual genotypes (WT vs TTNtvA or TTNtvZ) see Fig S7. * $P < 0.05$; ** $P < 0.01$; *** $P < 0.001$.

TTNtv impair cardiac performance during stress in rats and have adversely effect the heart in the general population

In young TTNtv rats (<8 months old) cardiac imaging showed features of concentric remodeling but normal LV mass and systolic function (Fig S11). In older rats (>1 year), TTNtv hearts were similar to controls although with a suggestion of slightly impaired systolic function (Fig 4a, Fig S12). While changes in cardiac morphology and function were mild in young mutant rats it was possible that this represented a compensated state as evidenced by the shift in cardiac metabolism (Fig 3) that is adaptive, at least in the short term²⁶. We examined cardiac function *ex vivo* and used a volume overload model to test the Frank-Starling response, which may be specifically impaired by genetic variation in TTN³³. Under basal conditions (LV end diastolic pressure, 5-10mmHg) TTNtv rat hearts

tended to have higher strain rates and LV developed pressures, perhaps reflecting compensatory metabolism (Fig 3) and signalling (Fig S10) but, when subjected to sequential volume overload stress, mutant heart function became increasingly impaired (Fig 4b). As observed previously^{34–36}, cardiac stress *ex vivo* activated mTORC1 signaling in control animals, which is an adaptive response. However, TTNtv hearts had elevated mTORC1 signaling at baseline and were not able to appropriately increase mTORC1 activity further when stressed (see Fig S10).

In the rat, TTNtv had mild effects on heart function irrespective of their position in the *Ttn* molecule but did not cause DCM. To explore the possibility that TTNtv in cardiac exons similarly affect the heart in human subjects, irrespective of disease status, we recruited 1,409 healthy individuals for detailed CMR studies of the heart in combination with *TTN* sequencing. We specifically focused our studies on the cardiac parameters of LV end diastolic volume (LVEDV) and ejection fraction (EF) that are used to define DCM³⁷ and also LV end systolic volume (LVESV) that is elevated in pre-DCM and predicts heart failure onset³⁸. In this cohort we identified 15 TTNtv (see Table S4; prevalence = 1.0%) in *TTN* exons (PSI > 15%), in keeping with our previous findings³ and the data from the ExAC Consortium¹¹. Truncations in *TTN* in our cohort and in the ExAC dataset were equally distributed across the *TTN* molecule (Fig S13).

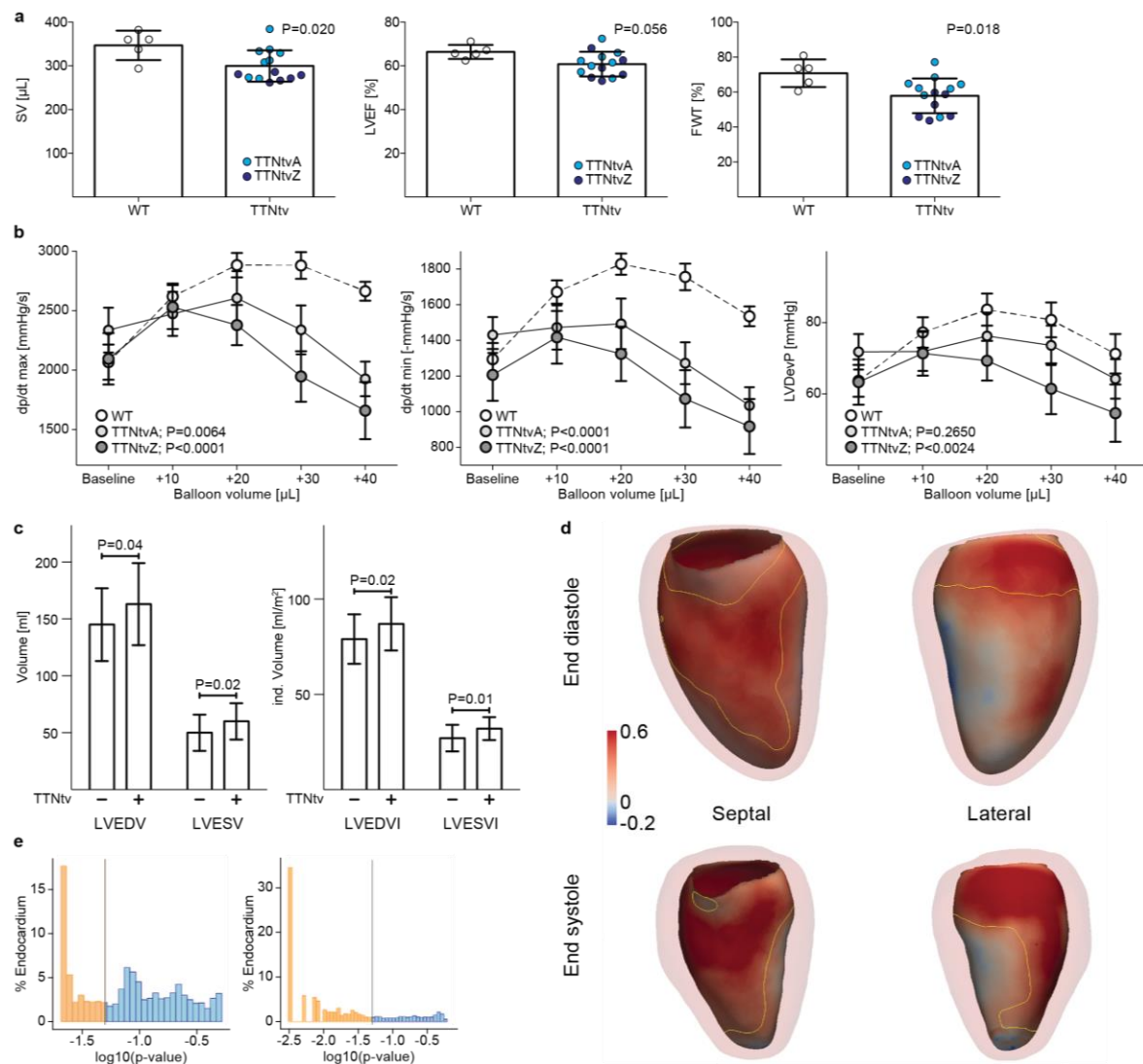


Fig 4. TTNtv in rats and humans adversely affect cardiac geometry and function. **a** SV (Stroke Volume), LVEF (Left Ventricular Ejection Fraction) and FWT (Fractional Wall Thickening) measured with CMR in 13-16 month old male WT (n=5) and TTNtv (TTNtvA, n=8; TTNtvZ, n=6) rats. Data are mean ± SD; [Statistical analysis by Student's *t* test]. For individual genotypes (WT vs TTNtvA or TTNtvZ) see Fig S12. **b** Measurements of *ex vivo* myocardial function during volume overload stress in 4 month old WT (n=9) and TTNtv (TTNtvA, n=8; TTNtvZ, n=8) rats. TTNtv hearts have mildly increased dp/dt max/min and LVDevP at baseline. Myocardial contraction rate, dp/dt max (mmHg/s); myocardial relaxation rate, dp/dt min (-mmHg/s); Left ventricle developed pressure, LVDevP (mmHg). Data are mean ± SEM; *P* values indicate statistical analysis by two-way analysis of variance [ANOVA]. **c** and **d**, human data. **c** Univariate analyses of left ventricular end diastolic volume (LVEDV), LVEDV indexed to body surface area (LVEDVI), left ventricular end systolic volume (LVESV) and LVESV indexed to body surface area (LVESVI). Healthy human individuals without a TTNtv in a cardiac exon (TTNtv-) are compared to healthy humans with a TTNtv (TTNtv+). Data are mean ± SD. [Mann-Whitney] **d** Computational modeling of cardiac geometry in healthy humans using 3D CMR. Positive standardised beta coefficients indicate where TTNtv genotype status (cardiac exons with PSI > 15%) is associated with enlargement of the LV cavity at end-diastole and end-systole. Septal and lateral *en face* projections are shown with an outline of the LV myocardium. The area enclosed by the yellow contour has a corrected *P* < 0.05 [mass univariate linear regression]. **e** The distribution of corrected *P* values (< 0.05 threshold shown) as a proportion of the endocardial surface is shown for both diastole (left panel) and systole (right panel) [mass univariate linear regression].

After genotype-blinded analysis of CMR data, we found that no individual from the general population with a TTNtv had imaging criteria for DCM, similar to our observations in the rat models and previous studies³. However, in univariate analyses TTNtv conferred a significant increase in absolute LV volumes and had more pronounced effects on volumes indexed to body surface area (Fig 4c). There was a non-significant trend for a lower LVEF in TTNtv+ individuals (LVEF (%): TTNtv+, 66 ± 5; TTNtv-, 63 ± 5; *P* = 0.06, Mann-Whitney). Given the multiple clinical and anthropometric variables that predict cardiac morphology and function, we built regression models for LVEDV, LVESV and LVEF

(see Methods and Table S5) and tested whether addition of TTNtv status improved model performance, which turned out to be the case (absolute beta values: LVEDV, +11.8mls (8.1%); LVESV +7.7 mls (15%); EF = -2.8% ($P < 0.03$ for all)). Of note, the effect size of TTNtv on cardiac parameters was much greater than the effect sizes of cardiovascular GWAS loci (e.g. systolic blood pressure; combined effect of all GWAS loci ~3%)^{39,40}.

To complement our 2D studies we collected an independent dataset of 3D CMR images and, blinded to genotype, performed atlas- and machine-based analyses of LV geometry with respect to TTNtv status^{41,42}. The 3D data show that TTNtv were associated with eccentric cardiac remodeling in healthy individuals. This was defined by outwards displacement of the endocardial border of the heart (Fig 4d,e and Supplementary video 1) in both systole (79% of total surface, $P < 0.05$) and diastole (47% of total surface, $P < 0.05$), in consensus with the 2D data.

Discussion

Here we studied the effects of TTNtv in patients with DCM, in the rat and in healthy humans to better understand these variants that represent the commonest genetic cause of DCM, yet are prevalent in the general population. At the molecular level, we found that TTNtv cause altered I-band splicing and position-independent NMD, which attenuates the synthesis of sarcomere-spanning *Ttn* isoforms. The NMD of the TTNtv allele that we observed in the F1 rat cross is the first demonstration of this effect and something we were not able to show previously using unphased human RNA-seq³. Distal truncations are associated with synthesis of carboxy-terminus truncated *Ttn* isoforms, whereas proximal TTNtv lead to translation of additional *Ttn* isoforms with alternative amino-termini. None of these additional isoforms were detected on protein gels, which suggests rapid degradation of these species (Fig S5). It was notable that, irrespective of their position in the *Ttn* molecule, both proximal and distal premature stop codons in the rat caused highly similar gene expression and translational signatures. While these molecular phenotypes are sufficient to impact heart function, it does not exclude additional, position-dependent effects that modify TTNtv penetrance in DCM where distal I-band and all A-band TTNtvs have the highest ORs.

The molecular phenotype due to TTNtv, which is reminiscent of cardiac adaptation to heart failure stimuli with a shift away from fatty acid metabolism^{26–28}, was associated with activation of the mTORC1 pathway that is also activated in familial DCM³⁰. We suggest that the metabolic (Fig 3) and signalling (Fig S10) changes in the TTNtv heart represent adaptive mechanisms^{26–28} and that the heart is maintained in a compensated state and therefore inflexible to further stress. This may explain why hemodynamic stress associated with pregnancy or possibly a second genetic factor may reveal TTNtv effects⁴³.

We found that TTNtv in constitutive exons throughout the *TTN* molecule, from the Z-disc to the M-line, are significantly associated with DCM. This has implications for interpretation of TTNtv in patients with DCM although A-band and distal I-band TTNtv have higher ORs than variants in other TTN domains, for reasons that remain unclear. In the general population, we show that TTNtv that were previously

thought to be of limited consequence⁴⁴ are associated with higher left ventricular volumes in 2D CMR analyses, which reflects underlying eccentric remodelling that was revealed using advanced 3D CMR techniques. The magnitude of effect of TTNtv on cardiac geometry in the general population may be large enough to adversely influence future cardiac events, which requires further study.

We note that TTNtv in exons that are expressed in the heart (PSI > 15%) are present in about 0.5% of individuals across all ethnicities^{3,11} and it may be that this variant class is of clinical relevance to ~35 million people, particularly if they are exposed to additional genetic or environmental cardiac stresses.

Acknowledgements

We thank all the patients and healthy volunteers for taking part in this research, and our team of research nurses across the hospital sites. We also thank Marion von Frieling-Salewsky for technical support. The research was supported by the Medical Research Council Clinical Sciences Centre UK, NIHR Biomedical Research Unit in Cardiovascular Disease at Royal Brompton & Harefield NHS Foundation Trust and Imperial College London, NIHR Imperial Biomedical Research Centre, British Heart Foundation UK (SP/10/10/28431, PG/12/27/29489), Wellcome Trust UK (087183/Z/08/Z, 092854/Z/10/Z, WT095908), Fondation Leducq, Tanoto Foundation, CORDA, National Medical Research Council (NMRC) Singapore, SingHealth Duke-NUS Institute of Precision Medicine, Rosetrees Trust, Health Innovation Challenge Fund (HICF-R6-373) funding from the Wellcome Trust and Department of Health, UK, Howard Hughes Medical Institute, the European Union EURATRANS award (HEALTH-F4-2010-241504), the Helmholtz Alliance ICAMED, European Union FP7 (CardioNeT-ITN-289600) to FM, Deutsche Forschungsgemeinschaft (SFB1002, TPA08 to W.A.L. & Forschergruppe 1054, HU 1522/1-1 to N.H.) and an EMBO Long-Term Fellowship (ALTF 186-2015) and Marie Curie Actions (LTFCOFUND2013, GA-2013-609409) to SvH. This publication includes independent research commissioned by the Health Innovation Challenge Fund (HICF), a parallel funding partnership between the Department of Health and Wellcome Trust. The views expressed in this work are those of the authors and not necessarily those of the Department of Health or Wellcome Trust. The RNA-seq and Ribo-seq data used in the manuscript can be obtained from <http://www.ebi.ac.uk/ena/data/view/ERP015402>.

References

1. Hershberger, R. E., Hedges, D. J. & Morales, A. Dilated cardiomyopathy: the complexity of a diverse genetic architecture. *Nat Rev Cardiol* **10**, 531–47 (2013).
2. Herman, D. S. *et al.* Truncations of titin causing dilated cardiomyopathy. *N. Engl. J. Med.* **366**, 619–28 (2012).
3. Roberts, A. M. *et al.* Integrated allelic, transcriptional, and phenomic dissection of the cardiac effects of titin truncations in health and disease. *Sci Transl Med* **7**, 270ra6 (2015).
4. Norton, N. *et al.* Exome sequencing and genome-wide linkage analysis in 17 families illustrate the complex contribution of TTN truncating variants to dilated cardiomyopathy. *Circ Cardiovasc Genet* **6**, 144–53 (2013).
5. Chauveau, C., Rowell, J. & Ferreiro, A. A Rising Titan: TTN Review and Mutation Update. *Human Mutation* **35**, 1046–1059 (2014).
6. Akinrinade, O., Koskenvuo, J. & Alastalo, T.-P. Prevalence of Titin Truncating Variants in General Population. *PLOS ONE* **10**, e0145284 (2015).
7. Akinrinade, Alastalo, T. -P. & Koskenvuo, J. W. Relevance of truncating titin mutations in dilated cardiomyopathy. *Clinical Genetics* n/a–n/a (2016). doi:10.1111/cge.12741
8. Robinson, E. B. *et al.* Genetic risk for autism spectrum disorders and neuropsychiatric variation in the general population. *Nat. Genet.* (2016). doi:10.1038/ng.3529
9. Hinson, J. T. *et al.* HEART DISEASE. Titin mutations in iPS cells define sarcomere insufficiency as a cause of dilated cardiomyopathy. *Science* **349**, 982–6 (2015).
10. Gramlich, M. *et al.* Stress-induced dilated cardiomyopathy in a knock-in mouse model mimicking human titin-based disease. *J Mol Cell Cardiol* **47**, 352–358 (2009).
11. Lek, M. *et al.* Analysis of protein-coding genetic variation in 60,706 humans. *bioRxiv* 030338 (2015). at <<http://biorxiv.org/content/early/2015/10/30/030338.abstract>>
12. Zou, J. *et al.* An internal promoter underlies the difference in disease severity between N- and C-terminal truncation mutations of Titin. *eLife* **4**, (2015).
13. Forrest, A. *et al.* A promoter-level mammalian expression atlas. *Nature* **507**, 462–470 (2014).
14. Schafer, S. *et al.* Alternative Splicing Signatures in RNA-seq Data: Percent Spliced in (PSI). *Curr Protoc Hum Genet* **87**, 11.16.1–11.16.14 (2015).
15. Ingolia, N., Ghaemmaghami, S., Newman, J. & Weissman, J. Genome-Wide Analysis in Vivo of Translation with Nucleotide Resolution Using Ribosome Profiling. *Science* **324**, 218–223 (2009).
16. Schafer, S. *et al.* Translational regulation shapes the molecular landscape of complex disease phenotypes. *Nature communications* **6**, 7200 (2015).
17. Kundaje, A. *et al.* Integrative analysis of 111 reference human epigenomes. *Nature* **518**, 317–330 (2015).
18. Guo, W. *et al.* RBM20, a gene for hereditary cardiomyopathy, regulates titin splicing. *Nat. Med.* **18**, 766–73 (2012).
19. Maatz, H. *et al.* RNA-binding protein RBM20 represses splicing to orchestrate cardiac pre-mRNA processing. *J. Clin. Invest.* **124**, 3419–30 (2014).
20. Hir, L., Izaurralde, Maquat & Moore. The spliceosome deposits multiple proteins 20-24 nucleotides upstream of mRNA exon-exon junctions. *Embo J* **19**, 6860–9 (2000).
21. Hir, L., Gatfield, Izaurralde & Moore. The exon-exon junction complex provides a binding platform for factors involved in mRNA export and nonsense-mediated mRNA decay. *Embo J* **20**, 4987–97 (2001).
22. Luo, W., Friedman, M. S., Shedden, K., Hankenson, K. D. & Woolf, P. J. GAGE: generally applicable gene set enrichment for pathway analysis. *BMC Bioinformatics* **10**, 161 (2009).
23. Kanehisa, M. & Goto, S. KEGG: kyoto encyclopedia of genes and genomes. **28**, 27–30 (2000).
24. Lai, L. *et al.* Energy metabolic reprogramming in the hypertrophied and early stage failing heart: a multisystems approach. *Circ Heart Fail* **7**, 1022–31 (2014).
25. Shibayama, J. *et al.* Metabolic remodeling in moderate synchronous versus dyssynchronous pacing-induced heart failure: integrated metabolomics and proteomics study. *PLoS ONE* **10**, e0118974 (2015).
26. Doenst, T., Nguyen, T. D. & Abel, E. D. Cardiac metabolism in heart failure: implications beyond ATP production. *Circ. Res.* **113**, 709–24 (2013).
27. Stanley, W. C., Recchia, F. A. & Lopaschuk, G. D. Myocardial substrate metabolism in the normal and failing heart. *Physiol. Rev.* **85**, 1093–129 (2005).
28. Schisler, J. C. *et al.* Cardiac energy dependence on glucose increases metabolites related to glutathione and activates metabolic genes controlled by mechanistic target of rapamycin. *J Am Heart Assoc* **4**, (2015).

29. Neubauer, S. The failing heart--an engine out of fuel. *N. Engl. J. Med.* **356**, 1140–51 (2007).
30. Yano, T. *et al.* Clinical impact of myocardial mTORC1 activation in nonischemic dilated cardiomyopathy. *Journal of molecular and cellular cardiology* **91**, 6–9 (2016).
31. Ramos, F. *et al.* Rapamycin reverses elevated mTORC1 signaling in lamin A/C-deficient mice, rescues cardiac and skeletal muscle function, and extends survival. *Science translational medicine* **4**, 144ra103 (2012).
32. Neishabouri, Hutson & Davoodi. Chronic activation of mTOR complex 1 by branched chain amino acids and organ hypertrophy. *Amino acids* **47**, 1167–82 (2015).
33. Ait-Mou, Y. *et al.* Titin strain contributes to the Frank-Starling law of the heart by structural rearrangements of both thin- and thick-filament proteins. *Proceedings of the National Academy of Sciences of the United States of America* **113**, 2306–11 (2016).
34. Sen, S. *et al.* Glucose regulation of load-induced mTOR signaling and ER stress in mammalian heart. *J Am Heart Assoc* **2**, e004796 (2013).
35. Shende, P. *et al.* Cardiac raptor ablation impairs adaptive hypertrophy, alters metabolic gene expression, and causes heart failure in mice. *Circulation* **123**, 1073–82 (2011).
36. Zhang, D. *et al.* MTORC1 regulates cardiac function and myocyte survival through 4E-BP1 inhibition in mice. *J. Clin. Invest.* **120**, 2805–16 (2010).
37. Mestroni *et al.* Guidelines for the study of familial dilated cardiomyopathies. Collaborative Research Group of the European Human and Capital Mobility Project on Familial Dilated Cardiomyopathy. *Eur Heart J* **20**, 93–102 (1999).
38. Vasan, R. S., Larson, M. G., Benjamin, E. J., Evans, J. C. & Levy, D. Left ventricular dilatation and the risk of congestive heart failure in people without myocardial infarction. *N. Engl. J. Med.* **336**, 1350–5 (1997).
39. Levy, D. *et al.* Genome-wide association study of blood pressure and hypertension. *Nat. Genet.* **41**, 677–87 (2009).
40. Newton-Cheh, C. *et al.* Genome-wide association study identifies eight loci associated with blood pressure. *Nat. Genet.* **41**, 666–76 (2009).
41. Marvao, A. de *et al.* Population-based studies of myocardial hypertrophy: high resolution cardiovascular magnetic resonance atlases improve statistical power. *J Cardiovasc Magn Reson* **16**, 16 (2014).
42. Bai, W. *et al.* A bi-ventricular cardiac atlas built from 1000+ high resolution MR images of healthy subjects and an analysis of shape and motion. *Med Image Anal* **26**, 133–45 (2015).
43. Ware, J. *et al.* Shared Genetic Predisposition in Peripartum and Dilated Cardiomyopathies. *New Engl J Medicine* **374**, 233–241 (2016).
44. Watkins, H. Tackling the achilles' heel of genetic testing. *Sci Transl Med* **7**, 270fs1 (2015).